Luminescence from Spherically and Aspherically Collapsing Laser Induced Bubbles

C. D. Ohl, O. Lindau, and W. Lauterborn

Drittes Physikalisches Institut, Universität Göttingen, Bürgerstraße 42-44, D-37073 Göttingen, Federal Republic of Germany

(Received 15 August 1997)

Single cavitation bubble luminescence is investigated. The cavitation bubbles are produced by focused laser light and collapse under the action of the ambient pressure. Both spherical and aspherical collapse is studied. Luminescence is observed in both cases, but only up to a mildly aspherical collapse. [S0031-9007(97)04982-X]

PACS numbers: 78.60.Mq, 47.55.Bx

Light emission from bubbles in liquids has received increased attention with the advent of single bubble levitation in sound fields [1]. In this Letter we present investigations of the light emission from single collapsing cavitation bubbles: single cavitation bubble luminescence (SCBL). Our method makes use of focused laser light to produce largely empty bubbles in a liquid, a method used earlier for cavitation bubble dynamics studies [2,3]. In contrast to acoustically driven bubbles in SBSL (single bubble sonoluminescence) [1] and MBSL (multibubble sonoluminescence) [4] experiments, laser induced bubbles do not need a sound field for a strong collapse and for light emission [5]. Laser induced bubbles can be made to collapse in adjustable aspherical geometry and thus may settle some questions about the origin of the luminescence. SCBL may also serve as a link between SBSL and MBSL in that the aspherical environment present in MBSL can be simulated in SCBL.

Figure 1 shows a sketch of the experimental arrangement used to investigate the bubble dynamics and the light emission during bubble collapse. A Q-switched Nd:YAG laser delivers single laser pulses of 8 ns width and up to 20 mJ energy at a wavelength of 1064 nm. The laser light is focused with an aberration minimized lens system into a cuvette filled with bidistilled water (85 mm $\times$ 85 mm $\times$ 75 mm, water at room temperature and air saturated). A focus angle of 25° places the focus 27 mm from the cuvette wall. This allows a nearly spherical geometry in the surrounding liquid for the investigated bubble sizes ranging from 0.8 mm to 1.5 mm in radius. Single bubbles are nucleated at the focus of the laser pulse when the dielectric breakdown threshold is reached, and a rapidly expanding plasma is formed. The recombining plasma gives rise to a gas- and vapor-filled bubble that grows to a maximum radius depending on the laser pulse parameters, in particular, pulse length and pulse energy [6]. The bubble collapses down to a minimum size until the compressed gas in the bubble leads to a rebound. During the collapse process, the bubble dissipates energy, mainly through emission of acoustic transients, and therefore reexpands to a smaller, second maximum bubble radius. The bubble dynamics is resolved with an image converter camera at 227.000 frames/s (Imacon 700, Hadland Photonics) with eight separate frames read out via a CCD (charge-coupled device) camera (1317 $\times$ 1013 pixel, 12 bit, Quantix, Photometrics). Each pixel of the CCD covers 6.25^2 μm^2 field of view.

To suppress the intense continuum light emission of the dielectric breakdown process, a gateable camera system with a high contrast ratio between the shuttered and opened state is needed. An intensified CCD system (PicoStar, LaVision) with a gated multichannel plate (MCP) and a gated photocathode serves this purpose. The gating times can be adjusted from 1 ms down to 120 ps. At the highest gain voltage of the MCP, one photoelectron is intensified to 150 counts. A fiber coupled slow scan CCD (384 $\times$ 286 pixel, 12 bit) integrates the light during the opening time. The optical imaging is done with a long distance microscope at 137 mm (73 mm in water, 5 mm cuvette glass thickness, and 59 mm in air) from the laser focus with 10$\times$ magnification, which gives 2.94^2 μm^2 field of view for each CCD pixel. The diameter of the aperture of the long distance microscope is 42 mm. The illumination with a photo flash (60 μs duration) and a ground glass plate is used either for the imaging of the bubble with the converter camera or, with considerable attenuation, for the photography of the bubble shape with the ICCD (intensified CCD).

The acoustic transients at bubble generation and at bubble collapse are recorded with a PVDF hydrophone having a bandwidth of 10 MHz (from CERAM AB,

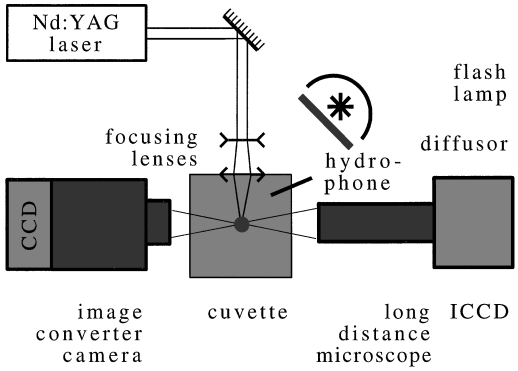

FIG. 1. Experimental arrangement for investigation of bubble dynamics and the emission of light of a laser induced cavitation bubble during collapse.

Sweden) and are stored on a transient recorder (TDS 784A, Tektronix) together with the monitor output of the image converter camera and the ICCD gate. The trigger for the individual devices are generated with a separate timing computer and a four-channel delay generator.

For the investigation of aspherical bubble collapse, a height adjustable rigid boundary of perspex is placed below the laser focus.

The technique for generation of cavitation through a laser induced dielectric breakdown allows the creation of a bubble in a highly reproducible way [2,3]. In the absence of a boundary, the bubble collapses spherically and emits a single shock wave [3]. Its dynamics can be very well modeled until the late stage of collapse with Gilmore's model [7].

Figure 2 shows an image of the luminescence which occurs during the spherical bubble collapse taken with the ICCD camera. The gating time was adjusted to 5 μs and an attenuated flash illuminates the bubble outline. The bright SCBL spot in Fig. 2 is centered. Light emission is only observed if the gating time of the ICCD covers the bubble collapse, which has been checked with the recorded hydrophone signal. Further, no measurable photon counts of the broad and intense continuum emission emitted from the dielectric breakdown are accumulated on the ICCD chip. This is a prerequisite for studying the spherical bubble collapse because the dielectric breakdown occurs at the same spatial position as the collapse and could lead to false interpretation. The maximum radius of the bubble, $R_{\max}$, in Fig. 2 was determined through Rayleigh's formula [8], Eq. (1), from the duration between bubble generation and bubble collapse $2T_c = 150.4$ μs to $R_{\max} = 0.813$ mm:

$$R_{\max} = \left(0.915\sqrt{\frac{\rho}{p - p_d}}\right)^{-1} T_c\,, \qquad (1)$$

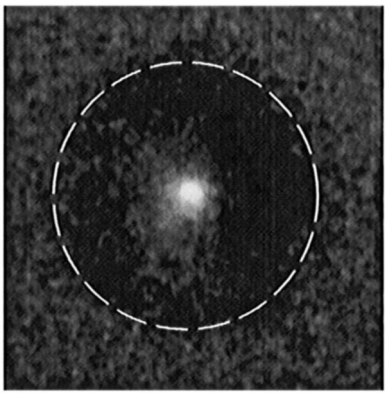

FIG. 2. ICCD image with a 5 μs shutter open time of a luminescing cavitation bubble with weak additional illumination from the front. The bubble appears dark on a bright background with the luminescence spot in the middle. During the shutter open time, the bubble wall collapses from the position marked with the dashed outline to a smaller bubble size, and therefore its shape becomes blurred. The size of the frame is 0.784 mm $\times$ 0.784 mm.

where $\rho = 998.2$ kg/m^3 is the density of the liquid, $p = 1$ bar is the ambient pressure, and $p_d = 0.0233$ bar is the vapor pressure at $T = 20$ °C.

The lower bound for the number of photons emitted can be roughly approximated: A single image of the luminescence with the same bubble size but without illumination gives 3.4×10^5 counts; a single photoelectron gives 64 counts at the adjusted voltage of the MCP. The quantum efficiency for the photocathode at 400 nm is 0.03. This efficiency is approximately valid for the luminescence, as has been checked with different cut-off filters. Further, the light is assumed to be emitted uniformly into the solid angle of 4π, and, with an ideal optics without reflection losses, the long distance microscope images 1/170th of the photons from geometrical considerations.

In this way, a lower bound of emitted photons during primary bubble collapse is determined to 30×10^6 photons for $R_{\max} = 0.813$ mm. In Fig. 3 the lower bound for the number of photons emitted for different maximum bubble sizes is plotted as dark squares. For each data point, ten luminescence events have been summed up onto the CCD chip and averaged. The dark signal has been subtracted from the images, and the number of photons have been estimated as above. A linear regression (dashed line in Fig. 3) gives a slope of 57×10^6 photons per mm maximum radius. There exists a threshold for the dielectric breakdown [6] whereby a bubble with a certain content of gas and vapor and a certain initial bubble wall velocity is formed. The resulting smallest $R_{\max}$ formed at the dielectric breakdown threshold (90% likelihood) was very close to 0.7 mm.

The ICCD camera takes a picture of the bubble illuminated by the light scattered from its interior. Assuming the luminescence event to be short, it freezes the bubble wall motion: A stop motion picture of the bubble at luminescence is photographed. From the diameter of the luminescence spot, an example of which is given in Fig. 2, we

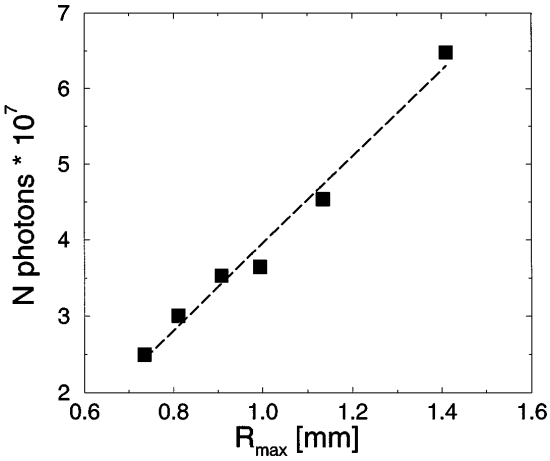

FIG. 3. Lower bound for the number of photons emitted during the primary bubble collapse for different maximum bubble radii.

can conclude that a bubble has a radius of 15 ± 6 μm for $R_{\max} = 0.813$ mm when luminescence occurs.

When the fluid flow in the surroundings of a bubble is disturbed, e.g., by a rigid boundary, the bubble dynamics before collapse is altered in a complex way. A simple description of the dynamics is given in the following: The bubble reduces its size, but the bubble wall nearer to the boundary is less strongly accelerated (as its flow is hindered by the boundary) than the radial flow from above. An indentation at the opposite bubble wall is formed and gives rise to an additional flow, apart from the pure radial one, in a direction towards the boundary. From momentum conservation [9], the bubble center accelerates during the collapse and moves towards the boundary. Considering a mirror bubble to fulfill the velocity boundary conditions on the rigid boundary, the attraction can be ascribed to the *secondary Bjerknes force* [10]. After the collapse, the bubble reexpands with a liquid flow, the *jet*, in a direction towards the boundary, forming a protrusion of the bubble which, for example, is visible in Fig. 4 (frames 4–7).

The dimensionless parameter $\gamma = s/R_{\max}$ helps to characterize the bubble collapse for different bubble radii $R_{\max}$ and distances s of the bubble center from the boundary. Varying the parameter γ from ∞, which is the spherical case, to a smaller value increases the influence of the boundary and thus the asphericity of the bubble collapse. Figure 4 consists of a combination of the two shared photographic devices. The frames 1–7 show the bubble dynamics for $\gamma = 5.9$. The bubble prior to collapse, frames 1 and 2, has a spherical shape. The bubble reaches minimum volume between frames 3 and 4, and the bubble center moves towards the boundary. The protrusion at the lower bubble wall is formed on a slower time scale than the bubble collapse, which is not resolved in greater detail. The liquid jet pushes the protrusion, whereas the main bubble body gains nearly spherical shape again.

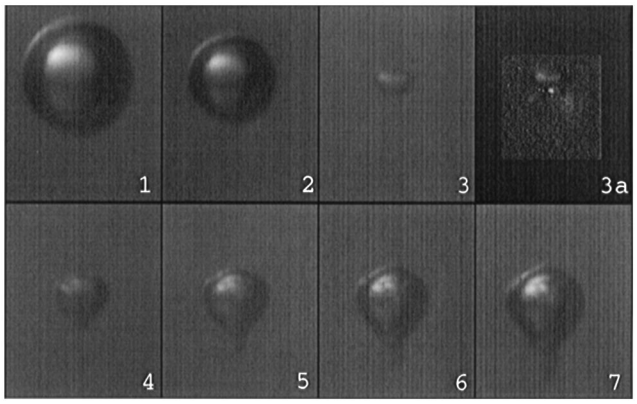

FIG. 4. Frames 1–7: bubble dynamics and light emission near a rigid boundary (not visible) placed $s = 4.9$ mm below the laser focus photographed with the image converter camera. The bubble reaches a maximum radius of $R_{\max} = 0.83$ mm, leading to $\gamma = 5.9$. The frames have 4.4 μs interframe time. Frame 3a: Blended picture of frame 3 and photograph of the light emission with the ICCD for a bubble with the same experimental parameters. The size of all individual frames is 1.56 mm $\times$ 1.25 mm.

Frame 3a of Fig. 4 is a blended image of the ICCD picture and frame 3. The cavitation luminescence is visible as the bright spot at the center of the lower bubble wall. The two imaging devices have photographed a different bubble, but the experimental parameters have not been altered. The high reproducibility of the experiment has been checked with the image converter camera, comparing the bubble dynamics for similar hydrophone signals and an unaltered boundary position. This is a precaution needed to compare the image of the ICCD and the images of the converter camera. Blending of the two frames has been controlled in two ways: First, the position of the light emission of the spherical bubble collapse was taken to determine the displacement of the luminescence in the aspherical case. With the displacement and the center of the bubble in frame one and the correct scaling of the ICCD image both images can be blended as done in frame 3a of Fig. 4. The blending was controlled to be correct with a second method. The attenuated flash, similar to that used in Fig. 2, illuminates the bubble shape. Thus, moving the ICCD image over the frames 5 to 7 of the image converter camera for the best visual match of the bubble shapes leads to the same displacement. The weak bright shades in frame 3a are due to the flash illumination of the bubble shape.

With this blending technique, we find that the light emission is located 103 μm below the laser focus. The light emission occurs at the very late stage of bubble collapse and is a single event. If multiple emission events would occur, a line or several discrete bright spots would have been imaged as the movement of the collapsing bubble would separate them spatially.

Calculation of the number of photons in the same way as in the spherical case gives 1.7×10^6 photons for $\gamma = 5.9$ and 5×10^5 photons for $\gamma = 4.7$. It is shown that the integrated luminescence decreases with smaller γ values, and no light emission from the bubble has been observed for γ below about 3.5. *Thus we can state that cavitation luminescence needs a highly spherical bubble collapse.*

Luminescence has been observed for all cavitation bubbles collapsing in spherical geometry. No luminescence has been observed during the second bubble collapse. The bubble rebounds after the first collapse to a smaller maximum radius due to the energy loss, mainly from emission of the shock wave. Thus the second collapse obviously is not strong enough to fulfill the conditions for light emission. The emission occurs at the geometrical center of the bubble and, as stated above, we assume that the shape of the emission is an image of the bubble scattering the light from its interior.

The photon numbers per luminescence event are at least an order of magnitude greater than observed in SBSL experiments. This is as expected, because the maximum bubble sizes for laser induced bubbles are 10 to 30 times larger compared to an SBSL experiment. Fitting measured

radius-time curves up to the second bubble collapse gives an approximate equilibrium bubble radius R_0 (bubble radius under static conditions). For the investigated maximum bubble radii the ratio $R_{\max}/R_0$ lies in the range between 5–10.

Jet theories [11] also rely on a nearly spherical collapse as then the jet velocities are higher when the jet forms. However, they are invalid for a perfectly spherical collapse, i.e., in the limit where asphericity turns to sphericity [12]. Aspherically collapsing bubbles luminesce at the bubble site of jet impact. This feature they share with shock compressed cylindrical bubbles in gels [13]. Time resolution in this experiment does not yet allow us to distinguish whether it is the instant of jet impact or the instant of bubble minimum when the luminescence flash is emitted. Even a framing rate of 20×10^6 frames/s [3] would not be high enough for γ larger than 3.5. For these cases, due to the increased sphericity, jet impact and bubble minimum are separated by less than 50 ns, the framing resolution of the camera.

Laser induced cavitation bubbles may become an intrinsic tool for further studies of luminescence accompanying bubble collapse. The very small size of SBSL bubbles at the moment of luminescence can be overcome with laser induced bubbles in SCBL. Another advantage is that no sound field is necessary as the bubble is fed with energy through the expanding plasma at dielectric breakdown. Therefore, experiments with laser induced bubbles do not have to cope with diffusion stability [14] and with the Bjerknes force threshold [15]. Moreover, systematic studies of luminescence from aspherical bubble collapse now open up a way to elucidate the mysterious connection between SBSL and MBSL [16]. Pictures of aspherically oscillating bubbles, but without luminescence, can be found in a recent publication [17]. SCBL can also be expanded to MCBL (multicavitation bubble luminescence). Two luminescence spots have been observed from two nearby cavitation bubbles, for instance.

This work has been supported by the Fraunhofer Gesellschaft. We thank the company, LaVision, Göttingen, for the loan of the ICCD camera, and the friendly support from Dr. Ahuja. We are especially grateful for the inspiring discussions with the members of the Cavitation and Sonoluminescence Group at the Drittes Physikalisches Institut, Göttingen.

[1] B. P. Barber, R. A. Hiller, R. Löfstedt, S. J. Putterman, and K. R. Weninger, Phys. Rep. **281**, 65 (1997); L. A. Crum and T. J. Matula, Science **276**, 1348 (1997).

[2] W. Lauterborn, Acustica **31**, 51 (1974); A. Vogel, W. Lauterborn, and R. Timm, J. Fluid Mech. **206**, 299 (1989); B. Ward and D. C. Emmony, J. Acoust. Soc. Am. **88**, 434 (1990); Y. Tomita and A. Shima, Acustica **71**, 161 (1990); A. Philipp and W. Lauterborn, Acustica **83**, 223 (1997).

[3] C. D. Ohl, A. Philipp, and W. Lauterborn, Ann. Phys. (Leipzig) **4**, 26 (1995).

[4] H. Kuttruff, Acustica **11**, 230 (1962); A. J. Walton and G. T. Reynolds, Adv. Phys. **33**, 595 (1984).

[5] A. A. Buzukov and V. S. Teslenko, JETP Lett. **14**, 189 (1971); A. G. Akmanov, V. G. Ben′kovskii, P. I. Golubnichii, S. I. Maslennikov, and V. G. Shemanin, Sov. Phys. Acoust. **19**, 417 (1974).

[6] C. A. Sacchi, J. Opt. Soc. Am. B **8**, 337 (1991); A. Vogel, S. Busch, and U. Parlitz, J. Acoust. Soc. Am. **100**, 148 (1996).

[7] F. R. Gilmore, "The Growth or Collapse of a Spherical Bubble in a Viscous Compressible Liquid," Hydrodynamics Laboratory, California Institute of Technology, Pasadena, California, Report No. 26-4, 1952.

[8] J. Rayleigh, Philos. Mag. **34**, 94 (1917).

[9] T. B. Benjamin and A. T. Ellis, Philos. Trans. R. Soc. London A **260**, 221 (1966).

[10] V. F. K. Bjerknes, *Fields of Force* (Columbia University Press, New York, 1906); T. G. Leighton, *The Acoustic Bubble* (Academic, London, 1994).

[11] A. Prosperetti, J. Acoust. Soc. Am. **101**, 2003 (1997); T. Lepoint, D. De Pauw, F. Lepoint-Mullie, M. Goldman, and A. Goldman, J. Acoust. Soc. Am. **101**, 2012 (1997).

[12] A look into the interior of a collapsing bubble to clarify whether a jet has formed or the sphericity has remained is still beyond the experimental state of the art.

[13] N. K. Bourne and J. E. Field, J. Fluid Mech. **244**, 225 (1992).

[14] S. Hilgenfeldt, D. Lohse, and M. P. Brenner, Phys. Fluids **8**, 2808 (1996); I. Akhatov, N. Gumerov, C. D. Ohl, U. Parlitz, and W. Lauterborn, Phys. Rev. Lett. **78**, 227 (1997).

[15] I. Akhatov, R. Mettin, C. D. Ohl, U. Parlitz, and W. Lauterborn, Phys. Rev. E **55**, 3747 (1997).

[16] L. A. Crum, J. Acoust. Soc. Am. **95**, 559 (1994); T. J. Matula, R. A. Roy, P. D. Mourad, W. B. McNamara III, and K. S. Suslick, Phys. Rev. Lett. **75**, 2602 (1995); T. J. Matula, R. A. Roy, and P. D. Mourad, J. Acoust. Soc. Am. **101**, 1994 (1997).

[17] Y. Tian, J. A. Ketterling, and R. E. Apfel, J. Acoust. Soc. Am. **100**, 3976 (1997).